



International Conference on Concentrating Solar Power and Chemical Energy Systems,  
SolarPACES 2014

## Design of a thermochemical storage system for air-operated solar tower power plants

S. Tescari<sup>a\*</sup>, S. Breuer<sup>a</sup>, M. Roeb<sup>a</sup>, C. Sattler<sup>a</sup>, F. Flucht<sup>a</sup>, M. Schmücker<sup>a</sup>, G. Karagiannakis<sup>b</sup>, C. Pagkoura<sup>b</sup> and A. G. Konstandopoulos<sup>b</sup>

<sup>a</sup> German Aerospace Center (DLR), Linder Hoehe, Cologne 51147, Germany

<sup>b</sup> Aerosol & Particle Technology Laboratory, Chemical Process & Energy Resources Institute Center for Research/Technology Hellas

---

### Abstract

The present study deals with the mechanical properties of structured reactors/heat exchangers, for high temperature heat storage via the cobalt oxide cyclic redox scheme. Two different structures (i.e. honeycomb and perforated block) and two different compositions (i.e. 100% cobalt oxide and 90 wt% cobalt oxide – 10 wt% aluminium oxide) were evaluated. During thermal cycling in the range of 800-1000°C, different loads were applied to the samples while monitoring their length variation. The integrity of the samples was assessed after every cycle. It was found that mechanical strength was substantially improved upon addition of 10 wt% aluminium oxide. The cobalt oxide/alumina composite presented lower maximal expansion during cycling and exhibited higher integrity, already after one thermal cycle.

Another important result is that, for both the honeycomb and the perforated block, the load decreases the over-all sample net expansion. Moreover, the perforated block exhibited lower expansion and better mechanical strength as compared to the honeycomb. Due to the better chemical performance expected to be achieved by the honeycomb structure, a compromise between these two structures has to be chosen (e.g. honeycomb structure with thicker walls). The results are used for building a thermochemical storage system prototype, implemented for the first time in an existing concentrated solar power facility (STJ).

© 2015 The Authors. Published by Elsevier Ltd. This is an open access article under the CC BY-NC-ND license (<http://creativecommons.org/licenses/by-nc-nd/4.0/>).

Peer review by the scientific conference committee of SolarPACES 2014 under responsibility of PSE AG

*Keywords:* Cobalt oxide composites, thermochemical storage, mechanical stability, prototype design

---

\* Corresponding author. Tel.: +49-2203-601-2402; fax: +49-2203-601-4141.

E-mail address: [stefania.tescari@dlr.de](mailto:stefania.tescari@dlr.de)

## 1. Introduction

The efficient storage of solar energy is a quite challenging issue. At present, several commercial systems are available storing the heat in its sensible form, using liquid [1,2] or solid storage media [3-6]. The latter is used for instance in air-operated solar tower power plants, like the Solar Tower in Jülich (STJ) [7]. During “charging” (on-sun operation) the hot air coming from the receiver is transferred to a ceramic storage assembly, with honeycomb-like structures, to provide a large heat exchange surface area between air and the solid storage medium [6,8]. During “discharging” (off-sun) operation the air flow is reversed: “cold” air passes through the storage medium and is heated up to a targeted temperature range before flowing to the power block.

The energy stored in this system, can be substantially increased by replacing the storage material with a material having a similar structure, but able to also participate in a reversible chemical reaction in the temperature range of interest. In this way, not only the sensible but also the chemical heat (of reaction) will be stored and released upon demand. This could offer higher energy density and possibility of storing the heat at higher temperature for longer periods. Several recent studies [9,10] deal with thermochemical heat storage, with the active material typically being incorporated in powder formulation. In this study, redox active (i.e. cobalt oxide based) material formulated as structured bodies will be analyzed.

To explore this concept, monolithic bodies made of a reactive material were prepared and the proof-of-concept feasibility was verified [11]. One of the key points of this system is the structural stability of the system [12]. For this reason, this paper focuses on the thermo-mechanical behavior of structured samples, when applying a load during their thermal/redox cycling. The results are used for the design and implementation of a thermochemical storage system prototype, to be implemented for the first time in an existing solar facility (STJ).

## 2. Reactive material shape

Two different monolithic bodies are considered in this study: a cylindrical block with few cylindrical holes passing through it (perforated block Fig. 1a), and a honeycomb structure with square channels (Fig. 1b). Both samples are cylindrical (about 3cm diameter and 3cm height). The perforated block, prepared with the aid of an in-house built hydraulic press, already described in [13] comprises of 12 holes, each with a diameter of 2mm. The honeycombs, prepared with the aid of a laboratory scale piston extruder from ECT GmbH, were calcined under air at 800°C for 2 hours. The calcined bodies had a cell density of 82 cells per square inch (cps), corresponding to a wall thickness of 0.67 mm and a hole dimension of 2.3mm. Relevant details on the sources of raw powders and the preparation of mixtures for extrusion are provided in another work [14].

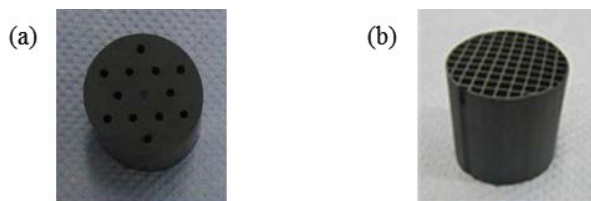


Fig. 1: Reactive material structured as (a) perforated block and (b) honeycomb.

## 3. Load tests

### 3.1. Experimental set-up

In order to evaluate the mechanical strength of the system, the samples were thermally cycled under mechanical loading, while applying variable loads. The experimental set-up allows to apply a load on the structured sample while subjected to thermal cycling. At the same time, potential dimensional changes are continuously recorded.

The experimental set-up is shown in Fig. 2. A ceramic plate located on the upper side of the sample allows a uniform distribution of the applied load. A constant pressure is applied on the top of this plate via a load-controlled testing machine. Relative position changes of the ceramic plate are recorded by means of an inductive extensometer. The dilatometry system is introduced into a HF furnace equipped with a SiC susceptor tube. Due to the experimental set-up, and in particular to the weight of the aluminum oxide plate placed above the sample, it is not possible to test loads lower than 8.6 kPa.

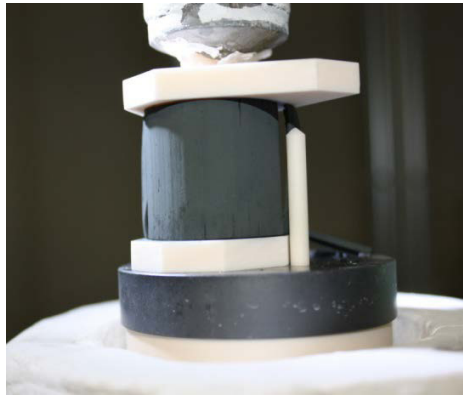


Fig. 2: Experimental set-up for load experiments.

The load to be applied during the experiments performed was chosen by considering the scaling up (i.e. system comprising of an assembly of such structured bodies). The prototype which will be installed in the STJ will comprise 500kg reactive material, shaped as a parallelepiped, with square base. The lower base of the storage (support surface) has to withstand the maximal load corresponding to the weight of the total material. The maximal load depends on the dimension of the support surface, which depends on the reactor shape and on the total volume of the reactor. Three reactor shapes are considered: cubic ( $H=L=W$ ), slim ( $H=2L=2W$ ) and flat ( $2H=L=W$ ). The total volume of the reactor depends on the bulk density. The perforated block shape (Fig. 1 a) has higher density compared to the honeycomb structure. This leads to a more compact storage system, corresponding to a smaller support surface. The maximum load, expected on this surface, is therefore higher.

Considering these maximal force, the loads to be applied to the small sample were calculated (Tab. 1).

Tab. 1: Load applied to the reactor base, depending on the material structure and the reactor shape

	$V_{Tot}$ (m <sup>3</sup> )	perforated block			honeycomb		
		0.18			0.51		
Prototype to be installed in STJ	Shape	L=2H	L=H	2L=H	L=2H	L=H	2L=H
	L (m)	0.71	0.56	0.45	1.01	0.80	0.63
	Load (g/cm <sup>2</sup> )	99	158	250	49	78	124
Small scale experiment	Applied load (kPa)	9.7	15.5	24.5	4.8	7.7	12.2

During the tests, the samples were cycled between 800 and 1000°C. The evaluation was initiated by applying the lowest load while the sample was heated up to 1000°C (10°C/min heating rate). The temperature was kept constant for 1h. Afterwards, the sample was cooled down (10°C/min cooling rate) in order to visually assess its integrity. The second (higher) load was then applied and the same procedure was repeated.

### 3.2. Results: perforated block

The results for a perforated block made of 90/10 wt% cobalt oxide/alumina composite are shown in Fig. 3. The dotted line shows the length change while applying the smallest load shown in Tab.1 (9.7 kPa). First the sample contracts (negative length change) due to the applied pressure. Afterwards, a slight expansion can be observed, most likely attributed to only-thermal effect. Once the reaction temperature is reached (about 900°C), the sample expands abruptly. The same behavior was shown in relevant literature studies [15,16] and was identified as thermal and chemical expansion. The maximal expansion at this stage was 0.8%. After this peak, the sample started to contract, although the temperature was still increasing, probably due to the applied load. A slight contraction continues during dwell time. When the temperature decreases, the sample contracts again abruptly. A slight change in the slope is visible, when crossing the redox reaction equilibrium temperature. The total contraction is about 0.5% of the initial length. This means that after the cycle, the sample shows a net expansion of about 0.3%.

A parallel study, focused on chemical and mechanical properties of cobalt oxide pellets [17], showed an increase of specimens' porosity and a shift to higher mean pore values after cycling. This explains the residual expansion of a cobalt oxide sample.

The sample length changes with a similar trend while applying higher loads (dashed and continuous lines in Fig. 3). Although the sample expansion is not strongly influenced by the applied load, the contraction becomes more pronounced for higher loads. As an effect of this, the net expansion disappears or becomes negative (net contraction) for higher loads. It is possible that the observed lower expansion in the vertical direction was compensated by a respective one in the lateral direction of the sample, however the setup employed here did not have the ability to verify such a phenomenon.

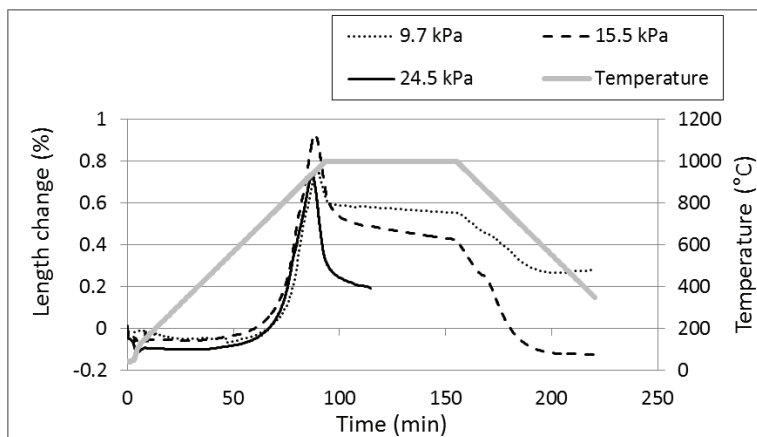


Fig. 3: Length change during a thermal cycle, applying different loads for perforated block made of 90% cobalt oxide - 10% aluminium oxide

Although some limited cracking became visible during the experiment (Fig. 4 a), the sample retained its macro-structural stability for the 3 step-load-increase cycles performed.

During the last cycle, after the end of the continuous line, an increasing load (up to 280kPa) was applied to the hot sample, in order to have information on the breakage pattern. As visible from Fig. 4 b, even when the sample broke, no detrimental collapse of its macro-structure was identified. Only a vertical slice was detached from the sample.

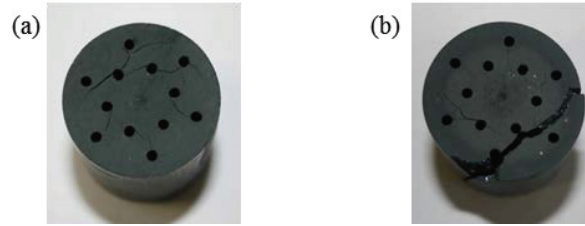


Fig. 4: Perforated block sample (a) after 3 cycles with the loads shown in Tab. 1 and (b) after the application of a much higher load

### 3.3. Results: honeycomb

The same experiments were carried out with the honeycomb structure (Fig. 1 b), having the same composition as the perforated block (90/10 wt% cobalt oxide/aluminina). As mentioned above, the lowest load applicable was 8.6 kPa, therefore (and based on Tab. 1 calculations) only 2 loads (8.6 kPa and 12.2 kPa) were tested and are presented in Fig. 5. The dashed line shows the length change by applying the lowest load. The sample contracts at the beginning upon heating and while applying the load. The contraction was followed by a first slow expansion (thermal-only effect) and subsequently, upon crossing the equilibrium temperature, a pronounced expansion occurred (chemical effect/reduction reaction dominated). The maximum expansion at this stage was 2.6%. Afterwards, the sample contracted slowly, due to the load, during the dwell time. In the cooling phase, the sample contracted initially slowly (thermal-only contraction) and then abruptly, upon occurrence of oxidation. The total contraction cannot compensate the previous expansion, leading to a 1.6% net expansion of the sample cf. its initial length.

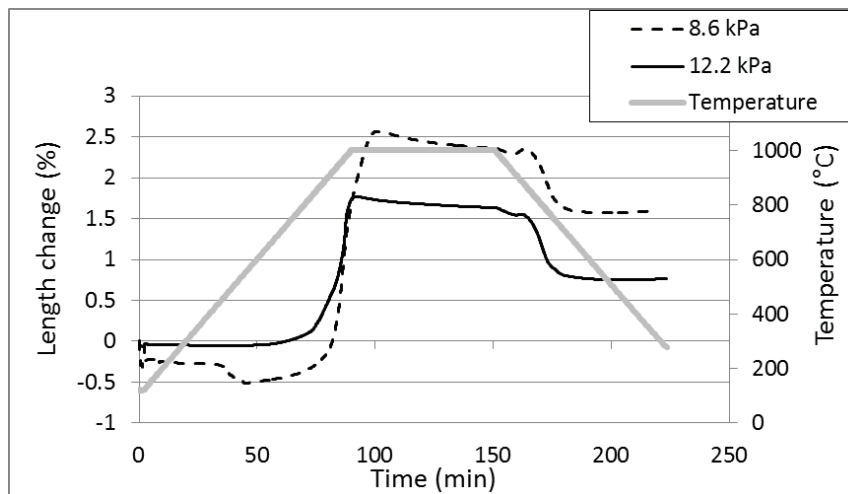


Fig. 5: Length change during a thermal cycle, applying different loads for a honeycomb made of 90% cobalt oxide - 10% aluminium oxide

Similar behavior, but with some clear differences, can be observed while applying the higher load (solid line in Fig. 5). The first contraction, due to the applied pressure, is visible only during the first cycle (low load conditions described above). When the same sample undergoes the second cycle (i.e. higher load), the length remains essentially constant until thermal expansion begins (at about 600°C). The higher load leads to a less profound expansion. The contraction during dwell and cooling phase follows an identical pattern with the respective one under low load conditions. As a result, the net expansion was measured to be much lower (0.85%) for this higher load.

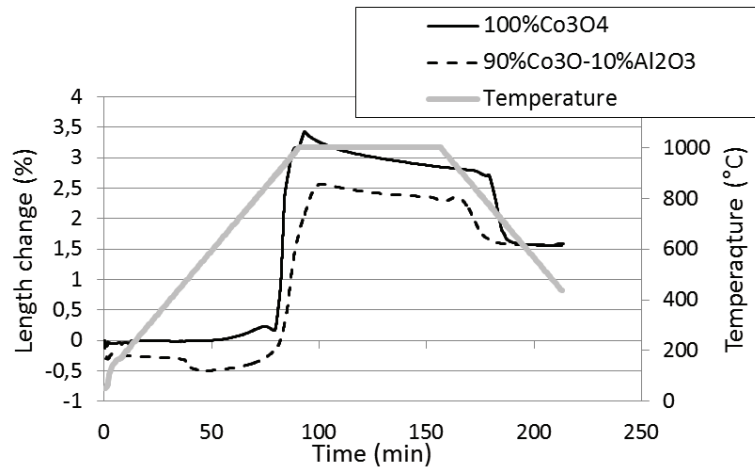


Fig. 6: Length change during a thermal cycle, for 8.6 kPa load for two honeycomb made respectively of 90% cobalt oxide - 10% aluminium oxide (dashed lines) and 100% cobalt oxide (continuous lines)

An identical honeycomb structure, with a different composition (pure cobalt oxide), was also evaluated, under the same operating conditions. Fig. 6 compares the results of the particular sample with the ones of the 90/10 wt% composite honeycomb for the lowest load applied (8.6 kPa).

With the exception of an initial contraction while the sample was still cold, the trend of the length change of the 2 samples is similar. The maximum expansion (calculated after the first contraction) was 3.5% for the pure cobalt oxide sample, cf. 3% for the composite one. At the same way, the thermal contraction was more profound for the pure sample, thus leading to almost the same net expansion after the cycle completion. A second important result shows the increase on the mechanical strength when adding 10% aluminium oxide to the composition of the sample. The honeycomb entirely made of cobalt oxide broke in three parts (Fig. 7 b), during the first cycle (load = 8.6 kPa) and was therefore not possible to test it with higher loads. Moreover, while extracting it from the experimental set up, it broke in several pieces. On the other hand, the composite sample sustained both loads (Fig. 7a), thus maintaining its macro-structural integrity, despite the appearance of a vertical crack in the sample. The same result was observed in a parallel study [14].

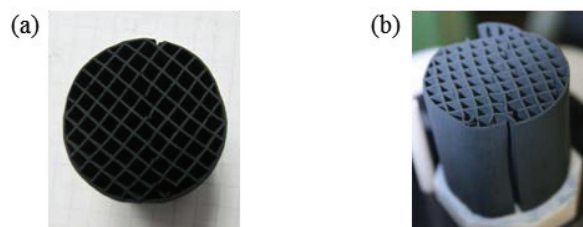


Fig. 7: Honeycomb samples made of (a) 90 wt% cobalt oxide – 10 wt% alumina and (b) 100 wt% cobalt oxide after testing

### 3.4. Comparison

Fig. 8 shows the comparison between the length change of the two composite structures (honeycomb vs perforated block) when applying a similar load. The denser structure (perforated block) exhibited a maximal

expansion which was 2.5 times smaller, compared to the honeycomb formulation (0.7% and 1.7% of the initial length respectively).

The most important difference between the samples was their mechanical stability, as it has to be expected. The perforated block structure was still integer after testing and it was probably able to stand many more cycles without breaking. The honeycomb structure, despite not broken into pieces, obtained a vertical crack after testing.

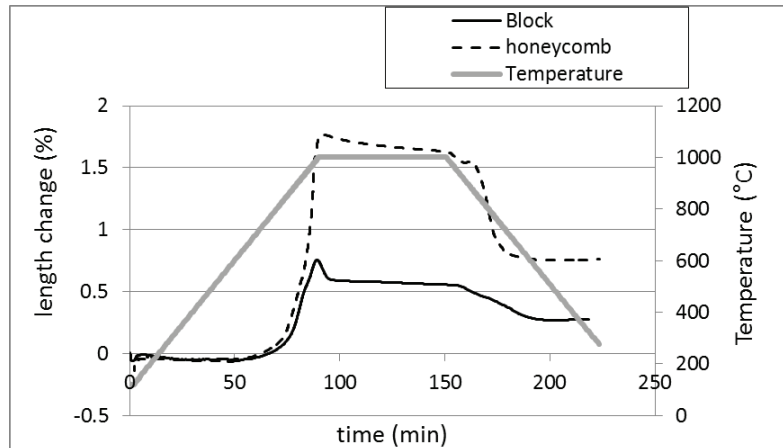


Fig. 8: Length change during a thermal cycle for the honeycomb sample (dashed lines) and for the perforated block (continuous lines)

Despite its lower mechanical strength, the honeycomb structure is expected to exhibit better characteristics regarding heat and mass transfer: a higher specific surface (i.e. higher gas-solid contact area) can in-principle improve the heat transfer between the gas and the solid while thinner walls allow better oxygen transfer through the material. Indeed, based on relevant multi-cyclic experimental campaigns related to cyclic redox performance assessment of the particular structures (i.e. measurements of oxygen released/consumed upon cyclic reduction/oxidation) not shown here for brevity, it was identified that the honeycomb composite showed a normalized redox performance (i.e.  $\mu\text{mol O}_2/\text{g Co}_3\text{O}_4$ ) that was approximately 50% of the maximum (i.e. corresponding to full reduction/oxidation) one. The redox performance remained essentially constant, with no apparent degradation phenomena identified, in the course of 112 cycles. On the other hand, the perforated block structure was subjected to 59 redox cycles and its average redox performance was measured at only 22% of the maximum theoretical value. Moreover, a cycle-to-cycle degradation on the order of 40% was identified when comparing redox activities achieved during the first 5 versus the last 5 cycles.

Naturally, if a structure combining better structural stability with an as low-as-possible loss of redox performance is to be pursued, a honeycomb with thicker walls than the one employed here could be an in-principle suitable option. Such an example is provided in Fig. 9. The particular structure has a wall thickness of 1.4 mm and a cell density of 46 cpsi. The particular structure is currently being evaluated in terms of both its redox performance and macro-structural/thermo-mechanical stability under variable load conditions.



Fig. 9: Honeycomb with thicker walls in order to achieve improved thermo-mechanical stability

#### 4. Reactor design

The chosen structure of reactive material (shown in Fig. 9) will be tested in the prototype reactor shown in Fig. 10 a. This prototype will be installed and tested in STJ. The storage module is divided into two, identical reactor chambers, which can work separately. This translates to a number of advantages. For example, it halves the load of the reactive material in the support base, it allows working under half load, when not enough energy is available, and it allows working with different conditions in the 2 chambers. In addition, the presence of 2 separate gas inlets guarantees a better uniformity of the gas velocity inside the reactor and lower pressure drop.

The reactive core is formed by honeycomb bricks, showing the same structure of the one in Fig. 9, but having a cubical shape of about 10cm side length. The cubical bricks are stacked one upon the other to form the two reactive parts, which occupy the center of the chambers.

The cubical shape of the whole reactive core was chosen in a parallel study, where a CFD model was developed to define the optimal shape and the operating conditions. The gas, entering from the top of the reactor (1 in Fig. 10), flows through a conical inlet (2), which guarantees a more uniform air distribution before it comes in contact with the reactive material. Some empty space is left above the reactive material, in order to leave the material free of expanding. As the reactors are designed vertically symmetric, there is effectively no difference for the direction of streaming.

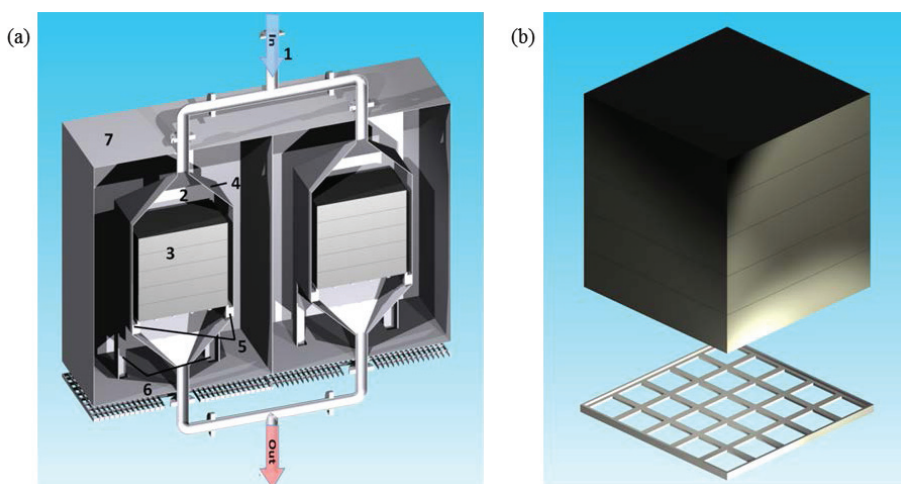


Fig. 10: Schematic of the prototype reactor which will be installed in the STJ (a) total reactor (sectional view); (b) reactive material block and grid structure

The reactive material is made of several cubical honeycomb bricks, stacked together to form 2 big cubical reactive blocks (3). Each reactive block (one each chamber), having a side of 0.5m, is placed on a grid holding structure (Fig. 10 b). This grid structure, made of high alloyed steel, is very stable and can withstand the weight of the honeycombs at operation temperature of 1000 °C. A second grid can be eventually added at half height of the reactive material, in order to decrease the load on the lower bricks. The grid is placed on a square metal plate (5), connected to the inner housing hull. The honeycombs are fixed horizontally via a small layer of insulation material, in the gap between the inner housing (4) and the honeycombs. This also absorbs possible dimension variation during the cycling. The inner housing has four feet (6), assembled at the 4 edges. Those are connected to the ground (shown here as a steel grating), and fixed there. The reactor chambers are housed with the outer hull (7), which is filled with high temperature insulating material. An opening device for the outer housing allows access to the honeycombs, if they need replacement or for visual inspection. The outer housing can be easily opened via an adequately large door, sealed with a rubber sealing, which can withstand continuous operation at 100 °C. The insulation will keep the outer temperature, to a rather low level.



## 5. Conclusion

The present study analyzed the mechanical properties of two monolithic bodies presenting different structures. A variable load was applied on the sample, during thermal cycling. The heating up of the element results in a first thermal expansion, up to the reaction temperature, followed by an abrupt chemical expansion. The dwelling and cooling down of the sample lead to a first slight contraction (thermal effect), followed by a fast contraction, upon occurrence of oxidation. In most of the cases, the contraction was smaller than the expansion, leading to a net expansion of the sample. For both the honeycomb and the perforated block, the net expansion was decreased by the load.

An important result shows that the mechanical strength can be improved, by adding 10% aluminium oxide to the composition of the sample. In addition, the composite sample exhibits a lower maximal expansion during cycling.

The perforated block shows lower expansion than the honeycomb and a better mechanical strength. Despite its lower mechanical strength, the honeycomb structure exhibits better characteristics regarding chemical conversion and a cycle-to-cycle degradation. In order to combine the 2 effects, a honeycomb with thicker walls than the one employed here, is currently being evaluated.

These results combined with the results obtained by a parallel CFD study on the complete reactor optimization, leads to the design of the prototype to be installed in the STJ, here presented. The installation of the prototype will begin in the near future.

## Acknowledgements

The authors would like to thank the European Commission for partial funding of this work within the Collaborative Project “Thermal energy storage for CSP plants: Redox Materials-based Structured Reactors/Heat Exchangers for Thermo-Chemical Heat Storage Systems in Concentrated Solar Power Plants (RESTRUCTURE) – contract n° 283015” under the Energy 2011.2.5.1 Call.

## References

- [1] Pacheco, J. E.; Bradshaw, R. W.; Dawson, D. B.; De la Rosa, W.; Gilbert, R.; Goods, S. H.; Hale, M. J.; Jacobs, P.; Jones, S. A.; Kolb, G. J.; Prairie, M. R.; Reilly, H. E.; Showalter, S. K.; Vant-Hull, L. L. Final Test and Evaluation Results from the Solar Two Project; Solar Thermal Technology, Sandia National Laboratories: P.O. Box 5800, Albuquerque, NM 87185-0703, 2002.
- [2] Steinmann, W.-D.; Eck, M., Buffer storage for direct steam generation. *Solar Energy* 2006, 80, (10), 1277-1282.
- [3] Laing, D.; Steinmann, W.-D.; Tamme, R.; Richter, C., Solid media thermal storage for parabolic trough power plants. *Solar Energy* 2006, 80, (10), 1283-1289.
- [4] Zanganeh, G.; Pedretti, A.; Zavattoni, S.; Barbato, M.; Steinfeld, A., Packed-bed thermal storage for concentrated solar power – Pilot-scale demonstration and industrial-scale design. *Solar Energy* 2012, 86, (10), 3084-3098.
- [5] Py, X.; Calvet, N.; Olives, R.; Meffre, A.; Echegut, P.; Bessada, C.; Veron, E.; Ory, S., Recycled Material for Sensible Heat Based Thermal Energy Storage to be Used in Concentrated Solar Thermal Power Plants. *Journal of Solar Energy Engineering* 2011, 133, (031008), 1-8.
- [6] Zunft, S.; Hänel, M.; Krüger, M.; Dreißigacker, V.; Göhring, F.; Wahl, E., Jülich solar power tower - experimental evaluation of the storage subsystem and performance calculations. In 16th Solar PACES International Symposium, Perpignan, France, 2010.
- [7] Hoffschmidt, B.; Fernández, V.; Pitz-Paal, R.; Romero, M.; Stobbe, P.; Tellez, F. In The development strategy of the HiTREC volumetric receiver technology – up-scaling from 200kWth via 3MWth up to 10MWel, Proceedings of 11th SolarPACES International Symposium on Concentrated Solar Power and Chemical Energy Technologies, Zürich, Switzerland, September 2002, 2002; Zürich, Switzerland, 2002.
- [8] Zunft, S.; Hänel, M.; Krüger, M.; Dreißigacker, V., High-temperature heat storage for air-cooled solar central receiver plants: a design study. In Solar PACES International Symposium, Berlin, Germany, 2009.
- [9] Schmidt, M.; Szcukowski, C.; Roßkopf, C.; Linder, M.; Wörner, A., Experimental Results of a 10 Kw High Temperature Thermochemical Storage Reactor Based on Calcium Hydroxide, *Applied Thermal Engineering*, 2014, 62, 553-559, 2014.
- [10] Neises, M.; Tescari, S.; de Oliveira, L.; Roeb, M.; Sattler, C.; Wong, B., Solar-heated rotary kiln for thermochemical energy storage. *Solar Energy* 2012, 86, (10), 3040-3048
- [11] Karagiannakis, G.; Pagkoura, K.; Zygianni, A.; Lorentzou, S.; Konstandopoulos, A.G.; (2013), *Energy Procedia*, SolarPACES, Las Vegas, USA
- [12] Wang, X.; Tian, W.; Zhai, T.; Zhi, C.; Bando, Y.; Golberg, D., Cobalt(Li,II) Oxide Hollow Structures: Fabrication, Properties and Applications, *Journal of Materials Chemistry*, 2012, 22, 23310-23326.

- [13] Pagkoura C., Karagiannakis G., Zygogianni A., Lorentzou S., Kostoglou M., Konstandopoulos A.G., Rattenburry M, Woodhead J.W. Cobalt oxide based structured bodies as redox thermochemical heat storage medium for future CSP plants. *Solar Energy* 2014; doi: 10.1016/j.solener.2014.06.034
- [14] Pagkoura C. Karagiannakis G, Zygogianni A., Lorentzou S., Konstandopoulos A.G., "Cobalt oxide based honeycombs as reactors/heat exchangers for redox thermochemical heat storage in future CSP plants" submitted paper n. 23507, SolarPACES, Sept. 16-19, Beijing, China
- [15] Chen X., Yu J., and Adler S. B., Thermal and Chemical Expansion of Sr-Doped Lanthanum Cobalt Oxide ( $\text{La}_{1-x}\text{Sr}_x\text{CoO}_{3-\delta}$ ). *Chem. Mater.* 2005, 17.4537-4546, doi:10.1021/cm050905h
- [16] Adler S.B., Chemical Expansivity of Electrochemical Ceramics, *Journal of the American Ceramic Society*, 2001, 84, 2117-2119.
- [17] Christos Agrafiotis\*, Stefania Tescari, Martin Roeb, Martin Schmücker, Christian Sattler, Exploitation of Thermochemical Cycles based on Solid Oxide Redox Systems for Thermochemical Storage of Solar Heat. Part 3: Cobalt Oxide Monolithic Porous Structures as Integrated Thermochemical Reactors/Heat Exchangers, 2014, submitted paper